

# FIRST STUDIES ON ERROR MITIGATION BY INTERACTION POINT FAST FEEDBACK SYSTEMS FOR FCC-ee\*

J. P. T. Salvesen<sup>†,1</sup>, F. Zimmermann, CERN, Geneva, Switzerland  
P. N. Burrows, <sup>1</sup>John Adams Institute for Accelerator Science, Oxford, UK

## Abstract

During operation, the Future Circular electron-positron Collider (FCC-ee) will be subject to vibrations from mechanical sources and ground motion, resulting in errors with respect to the closed orbit. To achieve physics performance, luminosity and beam lifetime must be kept to design specifications. To correct for errors at the interaction points (IPs), a fast feedback system is required. In this paper, we present the tolerances for the allowable beam offsets at the IPs and propose a fast feedback system to address these errors, with the methods of detecting and correcting errors discussed.

## INTRODUCTION

The Future Circular electron-positron Collider (FCC-ee) [1, 2] is a design study for a 91 km electron-positron collider based at CERN, Geneva. The collider is foreseen to operate with four Interaction Points (IPs), at four beam energies: 45.6 GeV (Z), 90 GeV (WW), 120 GeV (ZH) and 182.5 GeV (tt). The machine aims to be a luminosity-frontier, high energy lepton collider for precision physics. To maintain luminosity, beams must be kept in collision to high accuracy. Errors due to magnet vibrations, induced by ground motion [3] and other mechanical sources, must be suppressed. A fast IP feedback system is proposed to mitigate these errors. In the following, we discuss the performance requirements and potential input signals. Relevant parameters for the design of IP feedback for FCC-ee are listed in Table 1.

Table 1: FCC-ee Mid Term Review (MTR) Parameters [2]

Running mode	Z	WW	ZH	tt
Beam energy [GeV]	45.6	80	120	182.5
Bunches /beam	11200	1780	440	60
Hor. emit. $\epsilon_x$ [nm]	0.71	2.17	0.71	1.59
Vert. emit. $\epsilon_y$ [pm]	1.9	2.2	1.4	1.6
Hor. IP beta $\beta_x^*$ [mm]	110	220	240	1000
Vert. IP beta $\beta_y^*$ [mm]	0.7	1	1	1.6
$\sigma_z$ (BS) [mm]	15.5	5.41	4.70	2.17
Hor. BB $\xi_x$ [ $10^{-3}$ ]	2.2	13	10	73
Vert. BB $\xi_y$ [ $10^{-3}$ ]	97.3	128	88	134
Crab waist $k$ [%]	70	55	50	40
Lumi. /IP [ $10^{34} \text{ cm}^{-2} \text{ s}^{-1}$ ]	141	20	5.0	1.25

\* This work was supported by the European Union's Horizon 2020 Research and Innovation programme under grant no. 951754 (FCCIS).

<sup>†</sup> john.salvesen@cern.ch

## INTERACTION REGION DESIGN

The Interaction Region (IR) optics are based on a nano-beam, crab-waist collision scheme [4] with large Piwinski angle to allow  $\beta_y^*$  to be smaller than the bunch length without significant hourglass effect. Crab sextupoles are used to rotate the  $\beta_y^*$  at the IP as a function of the horizontal particle position, so that the vertical waists always align with the peak density of the opposing beam. Thereby, the crab sextupoles also suppress betatron resonances coupling the vertical and horizontal motion.

### Feedback Relevant Hardware

Luminosity monitors (“lumicals”) are situated at 1.1 m from the IP, on either side, with a target absolute measurement precision of  $1 \times 10^{-4}$  [5]. Attached to each lumical is a button Beam Position Monitor (BPM), fitted on the shared elliptical beam pipe. Further BPMs are located outside of the final focus quadrupole system and between the first and second quadrupole. A beamstrahlung (BS) dump is located 500 m downstream of the IP, and it is proposed to have a BS monitor along this photon line.

## PERFORMANCE REQUIREMENTS

Physics performance requires maintaining luminosity to a high precision. Beyond luminosity degradation, offsets at the IPs induce strong beam-beam deflections, negatively impacting the orbit, beam quality and lifetime. In particular, they lead to enhanced beamstrahlung and related longitudinal or transverse beam blow up. Offsets can also drive betatron resonances further disrupting the beam. Particle tracking is used to simulate the impact of offsets in transverse position or slope at the IP.

Previous studies, using CDR beam parameters, but assuming 4 IPs, at the Z working point concluded that a vertical orbit at IP should be maintained to within  $0.05\sigma_y$  [6]. Luminosity and beam distributions were considered. A combination of density contour plots, analysing the beam distributions in action space, and frequency map analysis, to identify the important excited resonances, were used to analyse the sensitivity to offsets. Refined studies for the current configuration are still being carried out; the tolerances are expected to be close to the past results.

## POTENTIAL FEEDBACK SIGNALS

To identify IP offsets during beam operation, a number of signals are available: BPM signals, luminosity and BS radiation. Each signal poses different challenges, and has different discrimination power for detecting offsets.

## Simulation Description

Single bunch crossings are simulated using the Particle In Cell solver GUINEA-PIG (GP) [7, 8].

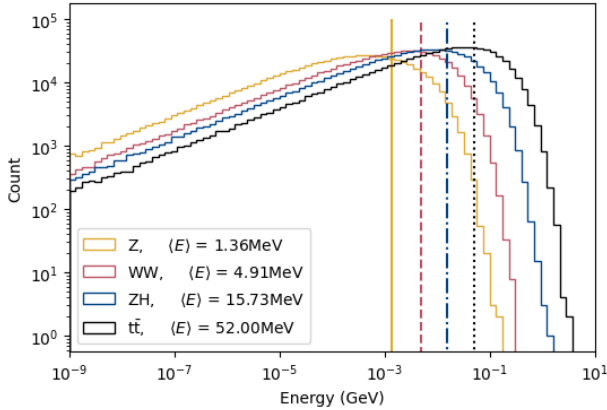


Figure 1: Beamsstrahlung spectra for the 4 different operating modes of FCC-ee, with zero offset.

Due to the log-concave form of the BS spectrum, spanning several orders of magnitude (shown in Fig. 1), a large number of macroparticles ( $10^5$ ) are used. For each offset, 50 bunch crossings are simulated with different random seeds. For all plots, error bars correspond to statistical errors over these 50 seeds. The initial particle distribution is obtained by applying an analytic crab waist transform to a Gaussian distribution based on equilibrium (BS) bunch sizes, according to the Hamiltonian

$$H_{CW} = kxy'^2 \quad (1)$$

, where  $x$  and  $y'$  are horizontal position and vertical slope at the IP, and  $k$  is the strength of the crab waist (see Table 1). A perfect crab waist is achieved with  $k = 1/\theta_c$ , where  $\theta_c$  is the full crossing angle, 30 mrad for FCC-ee.

## BPM Signals

During the bunch crossing, the beams impart a beam-beam kick on each other's centroid motion, typically, for small offsets, approximated by a linear deflection according to

$$\Delta a' \approx \pm \frac{2\pi\xi_a}{\beta_a^*} \Delta a \quad a \in x, y \quad (2)$$

, where the strength of the kick is linearly dependant on the beam-beam tune shift. For FCC-ee, the high vertical beam-beam tune shifts make a deflection measurement signal feasible at downstream BPMs. In the horizontal plane, the tune shifts are markedly lower, except for the  $t\bar{t}$  working point.

The outgoing beam deflection was simulated as a function of the offset, using GP. Results are shown in Fig. 2. This output corresponds only to the outgoing centroid angle from the IP, and does not consider the possible influence of the experimental solenoid, nor of any subsequent compensation solenoid magnets or downstream quadrupoles.

The leading choice of BPM for a fast feedback system is the lumical BPM at 1.1 m from the IP. This BPM is located

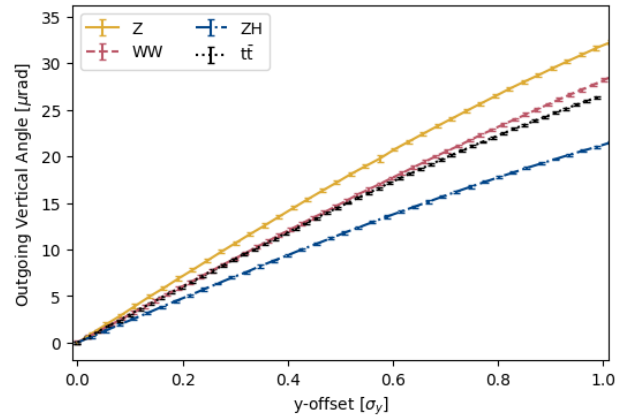


Figure 2: Outgoing centroid beam deflection as a function of incident beam offset for the vertical plane.

within the solenoid field, prior to the final focus quadrupoles, and strongly mechanically linked with the IP, reducing the complexity of calculating the IP offsets from the BPM measurements. However, at only 1.1 m from the IP, resolving offsets of a few percent of the RMS beam size implies a requirement of sub-micron resolution for this BPM, which may represent a technical challenge, also taking into account impedance constraints. Alternatively, using BPMs further downstream relaxes the BPM resolution requirement, but introduces potential errors from the final-focus quadrupoles. Furthermore, assuming an upper bound of turn-by-turn feedback equal to the revolution frequency (3.3 kHz) it would be possible to improve position information by averaging across multiple bunches.

## Luminosity Signal

Luminosity as measured by the lumical represents a relatively slow signal. To achieve the absolute luminosity reading, the calorimeter integrates over a number of crossings. Fast luminosity monitors, using the radiative Bhabha losses are under investigation. These may allow for bunch-by-bunch relative luminosity measurements, as operated at SuperKEKB [9]. Results of GP simulations of Luminosity change with offset are shown in Fig. 3, and key values are summarised in Table 2.

Table 2: Offset Tolerances for Luminosity from GP

	% Luminosity	Z	WW	ZH	$t\bar{t}$
<b>Lumi. /IP</b> [ $10^{34} \text{ cm}^{-2} \text{ s}^{-1}$ ]	MTR	141	20	5.0	1.25
	100%	141.5	20.5	5.0	1.48
<b>x-offset</b> [m]	99%	2.18	3.83	2.90	4.72
	95%	4.97	8.70	6.73	10.3
<b>y-offset</b> [nm]	99%	4.96	7.62	5.03	6.97
	95%	11.2	17.3	11.4	16.0

Luminosity also presents the challenge of being a scalar signal. As such, there is no direct information on which direction to drive the beam for correction. This directional information can be obtained from luminosity signals if the

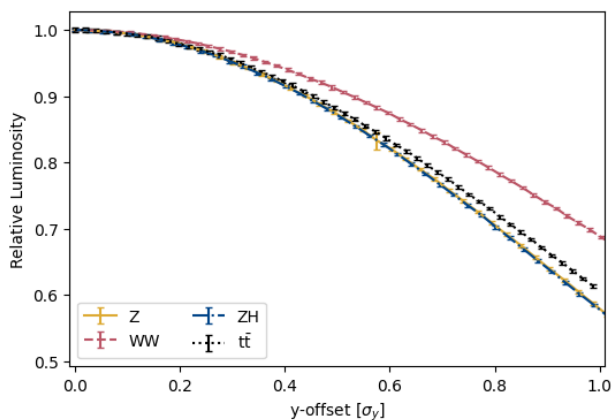


Figure 3: Luminosity as a function of incident beam offset for the vertical plane.

beam is driven: the dithering approach, currently employed at SuperKEKB in the horizontal plane [10, 11] and previously at SLC in the vertical plane [12]. This approach however entails sacrificing luminosity by dithering the beam.

### Beamstrahlung Signal

The use of beamstrahlung radiation is an enticing option, as the signal is a direct measure of the opposing beam, not a convolution of the separation of both beams. Both the position of the radiation (here described by the angle of emission) and the total power can be measured. However, this signal is difficult to measure due to the intense radiation power, reported in Table 3. Results of GP simulations of BS angle and power with offset are shown in Figs. 4 and 5.

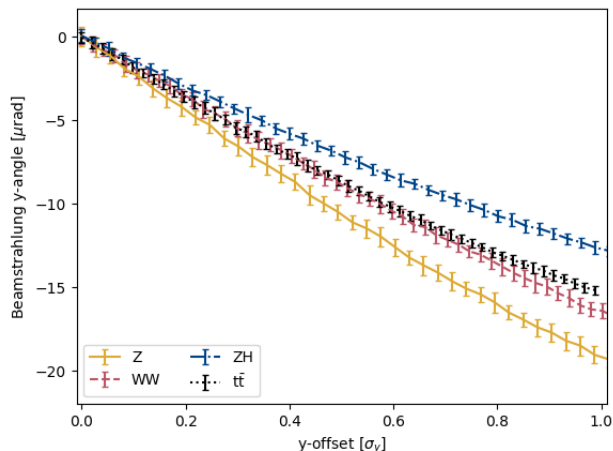


Figure 4: Beamstrahlung angle as a function of incident beam offset for the vertical plane.

Table 3: Beamstrahlung Power per Direction

BS Power [kW]	Z	WW	ZH	tt
GP nominal	229	95.5	63.6	40.2
GP 1σ x-offset	239	94.0	63.4	29.0
GP 1σ y-offset	299	120.2	84.5	54.3

Beamstrahlung signals show much clearer trends with offset in the vertical plane, with the exception of the tt working point, where the much smaller Piwinski angle and high beam-beam tune shifts leads to significant changes in BS radiation with horizontal offset. In the vertical plane, BS photon angle is zero for zero offset. In the horizontal plane, the crab collision scheme with large crossing angle causes an energy dependence of the initial angle. At nominal collision the horizontal angles are 36.9, 18.8, 14.2 and 5.1 μrad for the Z, WW, ZH and tt working points respectively.

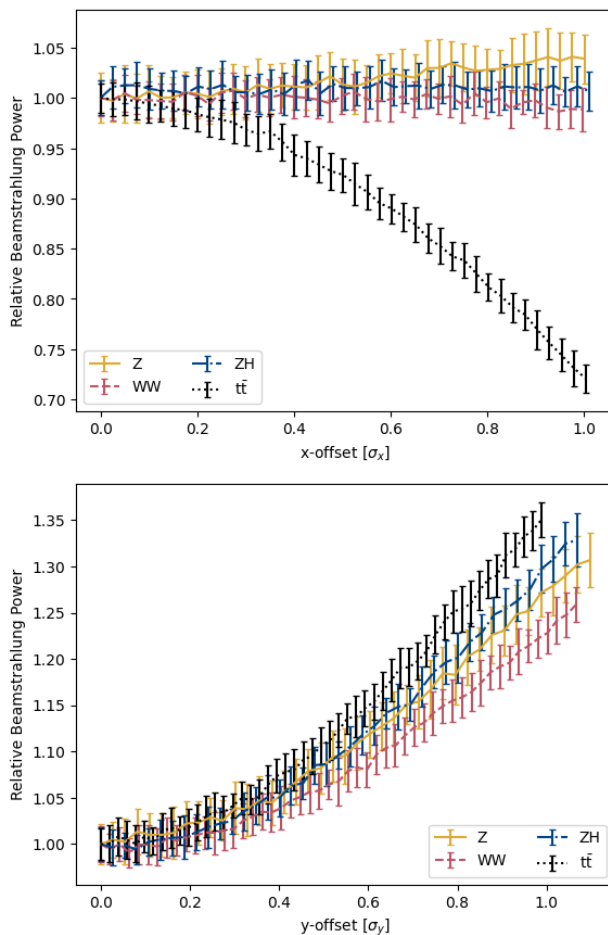


Figure 5: Beamstrahlung power as a function of incident beam offset in both the horizontal and vertical planes.

## CONCLUSION

Multiple signals are available to identify offsets at the interaction points of FCC-ee. Interesting technical challenges are encountered for all signals due to the required processing speed and resolution. These challenges include: high radiation power, impedance constraints, and the complex structure and space limitations of the FCC-ee machine detector interface.

## ACKNOWLEDGEMENTS

We thank A. Ciarna and V. Gawas for helpful discussion on GUINEA-PIG, and D. Shatilov for his input on performance requirements.

## REFERENCES

- [1] M. Benedikt *et al.*, “FCC-ee: the lepton collider: Future Circular Collider conceptual design report volume 2”, *Eur. Phys. J. Spec. Top.*, vol. 228, pp. 261–623, 2018.
- [2] B. Auchmann *et al.*, “FCC Midterm Report”, 2024. doi:10.17181/zh1gz-52t41
- [3] E. Montbarbon *et al.*, “First studies of final focus quadrupoles vibrations of the z lattice of FCC-ee”, in *Proc. IPAC’23*, Venice, Italy, 2023, pp. 731–733. doi:10.18429/JACoW-IPAC2023-MOPL077
- [4] M. Boscolo *et al.*, “The status of the interaction region design and machine detector interface of the FCC-ee”, in *Proc. IPAC’23*, Venice, Italy, 2023, pp. 256–259. doi:10.18429/JACoW-IPAC2023-MOPA091
- [5] M. Dam, “Challenges for FCC-ee luminosity monitor design”, *The European Physical Journal Plus*, vol. 137, p. 81, 1 2022. doi:10.1140/epjp/s13360-021-02265-3
- [6] D. Shatilov, “Large footprint with 4 ip (can cross half-integer), discussion and mitigation”, in *FCC-ee Optics Design Meeting*, 2019. [https://indico.cern.ch/event/835526/contributions/3502567/attachments/1883194/3103414/shatilov\\_4IP\\_footprint.pdf](https://indico.cern.ch/event/835526/contributions/3502567/attachments/1883194/3103414/shatilov_4IP_footprint.pdf)
- [7] D. Schulte, “Beam-beam simulations with GUINEA-PIG”, 1999.
- [8] GUINEA-PIG++, 2024. [https://abpcomputing.web.cern.ch/codes/codes\\_pages/Guinea-Pig](https://abpcomputing.web.cern.ch/codes/codes_pages/Guinea-Pig)
- [9] C. Pang *et al.*, “A fast luminosity monitor based on diamond detectors for the SuperKEKB collider”, *Nucl. Instrum. Methods Phys. Res., Sect. A*, vol. 931, pp. 225–235, 2019. doi:10.1016/j.nima.2019.03.071
- [10] Y. Funakoshi *et al.*, “Interaction Point Orbit Feedback System at SuperKEKB”, in *Proc. IPAC’15*, Richmond, VA, USA, May 2015, pp. 921–923. doi:10.18429/JACoW-IPAC2015-MOPHA054
- [11] Y. Funakoshi *et al.*, “Recent Progress of Dithering System at SuperKEKB”, in *Proc. IPAC’17*, Copenhagen, Denmark, May 2017, pp. 1827–1829. doi:10.18429/JACoW-IPAC2017-TUPIK059
- [12] L. Hendrickson *et al.*, “Luminosity optimization feedback in the SLC”, Rep. SLAC-PUB-8027, 1999.